Available online at www.sciencedirect.com
SCIENCE DIRECT
Journal of Power Sources 156 (2006) 712–718
JOURNAL OF POWER SOURCES
www.elsevier.com/locate/jpowsour

Influence of temperature and electrolyte on the performance of activated-carbon supercapacitors

Ping Liu [a,*], Mark Verbrugge [b], Souren Soukiazian [a]

[a] *HRL Laboratories, LLC, 3011 Malibu Canyon Road, Malibu, CA 90265, USA*
[b] *Materials and Processes Lab, 480 106 224, General Motors Corporation, R&D Center, 30500 Mound Road, P.O. Box 9055, Warren, MI 48090-9055, USA*

Received 6 April 2005; accepted 17 May 2005
Available online 27 June 2005

Abstract

For hybrid electric vehicle traction applications, energy storage devices with high power density and energy efficiency are required. A primary attribute of supercapacitors is that they retain their high power density and energy efficiency even at −30 °C, the lowest temperature at which unassisted starting must be provided to customers. More abuse-tolerant electrolytes are preferred to the high-conductivity acetonitrile-based systems commonly employed. Propylene carbonate based electrolytes are a promising alternative. In this work, we compare the electrochemical performance of two high-power density electrical double layer supercapacitors employing acetonitrile and propylene carbonate as solvents. From this study, we are able to elucidate phenomena that control the resistance of supercapacitor at lower temperatures, and quantify the difference in performance associated with the two electrolytes.

Keywords: Activated carbon; Nonaqueous electrolyte; Capacitor; Electrical double layer; Temperature dependence

1. Introduction

Electrochemical supercapacitors based on activated carbon have the potential to become energy-efficient, low-cost, high-power devices for automotive applications [1–3]. In these devices, charge is stored in the electrical double layer with effectively no accompanying chemical or Faradaic reactions, leading to very high power capabilities and long cycle life. Non-aqueous electrolytes are used in current commercial products so that higher voltages and energy densities can be achieved. These supercapacitors are constructed with (activated) carbon electrodes, aluminum foil current collectors, low-cost organic solvents, and immediately available salts. The two open questions with respect to cost are (1) Can the cost of activated carbon be brought down sufficiently and (2) can less expensive salts (ideally non-fluoride based, thereby reducing cost) be identified?

Prior to using supercapacitors in automotive applications, issues related to performance and abuse tolerance must be addressed. Commercial supercapacitors have been tested using various protocols and characterized with electrochemical techniques, such as constant-current potentiometry, constant-power excitation, cyclic voltammetry, and electrochemical impedance spectroscopy [3–4]. The overall resistance and capacitance are two important values that can be used to characterize the performance of the cell. Recent work on the contributions of different components in the supercapacitor to the internal resistance has indicated that electrolyte ionic transport and resistance at the carbon-electrode/aluminum-current collector interface are primary contributors to the cell resistance [5]. Portet et al. [6] have achieved a significant reduction in resistance and simultaneous increase in power density by pre-treating the aluminum current collector to render it microporous. There are also intensive efforts directed at developing advanced component materials. New activated carbons have the promise of low cost [7–8], and novel ammonium salts may

* Corresponding author. Tel.: +1 310 317 5474.
E-mail address: pliu@hrl.com (P. Liu).

0378-7753/$ – see front matter © 2005 Elsevier B.V. All rights reserved.
doi:10.1016/j.jpowsour.2005.05.055

lead to supercapacitors with higher voltages, yielding larger power and energy densities [9].

The abuse tolerance of supercapacitors, particularly those formulated with acetonitrile (ACN), remains a source of concern for end users, particularly in the automotive community wherein large capacitor modules would be required for traction applications. The concern is primarily due to the volatility of the organic solvent and unwanted species generated during combustion of ACN. Previous evaluations of supercapacitors have established that ACN-based electrolytes yield high energy and high power performance [3]. There has been an intensive search underway to identify an alternative solvent, with the most promising alternative being propylene carbonate (PC). However, it is known that PC-based electrolytes usually have a lower conductivity than those based on ACN, which adversely impacts the power capability and energy efficiency of the capacitor. Several recent publications have discussed the effect of solvent properties on the characteristics of laboratory-built electrochemical capacitors. This investigation complements those in Refs. [10–13] by providing detailed performance data as a function of temperature and clarifying the role of the solvent in determining the cell behavior. We perform a direct comparison between two otherwise identical supercapacitors built with ACN and PC based electrolytes. We examine the evolution of resistance and capacitance of the two supercapacitors with temperature. General discussions on the effect of temperature on supercapacitor performance can be found in Conway's book [14]. The present work aims to identify the underlying limiting factors of supercapacitor performance for the two electrolyte systems.

2. Experimental

The capacitors for this study were built by Nesscap Co., Ltd. The ACN and PC based supercapacitors had nominal capacitances of 100 F, and maximum voltages of 2.7 and 2.5 V, respectively. Electrochemical tests were performed on an Arbin BT2000 battery testing system (Arbin Instruments, College Station, TX). Generally, data acquisition rates of approximately 1 point per 100 ms were used. Tests were conducted at temperatures between −30 and 45 °C. Temperature control was provided by a Tenney environment chamber (Model Tenney20, Lunaire, Williamsport, PA). Prior to a test, the supercapacitor was allowed to equilibrate at a given temperature for 4 h.

Ragone plots were obtained by performing a series of increasing constant discharge power tests on the supercapacitors. Prior to the discharge, the supercapacitors were charged using a low current (1 A) to the maximum voltage and held at that voltage for 30 min to ensure full charging of the supercapacitors. The discharge voltage limits are set between the maximum voltage and half of its value.

A series of energy-measurement tests was performed to estimate the resistance and capacitance values of the supercapacitors. At each temperature, the ACN-based capacitor was discharged to 0 V and held at that voltage for 300 s. It was subsequently charged to a preset potential of 1.7 V at a constant current of 40 A, followed by an open-circuit rest for 180 s. The supercapacitor was then discharged to 0 V at a constant current of 2 A. This sequence was repeated for a series of preset potentials at 0.1 V increments from 1.8 to 2.4 V. Similar tests were performed on the PC-based capacitor, with the maximum voltage ranging from 1.5 to 2.2 V. For temperatures above 0 °C, the PC-based capacitor charging and discharging currents were 20 and 2 A, which were reduced to 5 and 2 A for lower temperatures.

3. Results and discussion

An initial characterization of the supercapacitors is provided by the Ragone plots shown in Fig. 1. A remarkable insensitivity of performance to temperature is observed for the ACN-based capacitor. Lowering the temperature down to 0 °C has virtually no effect on the cell performance. At

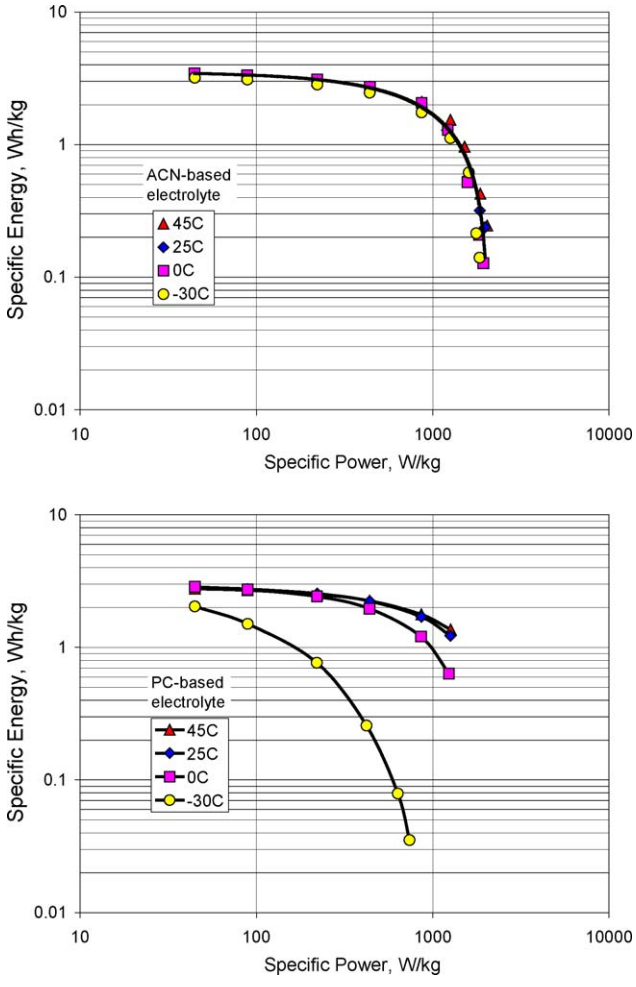

Fig. 1. Ragone plots for ACN (top) and PC (bottom) based capacitors at different temperatures.

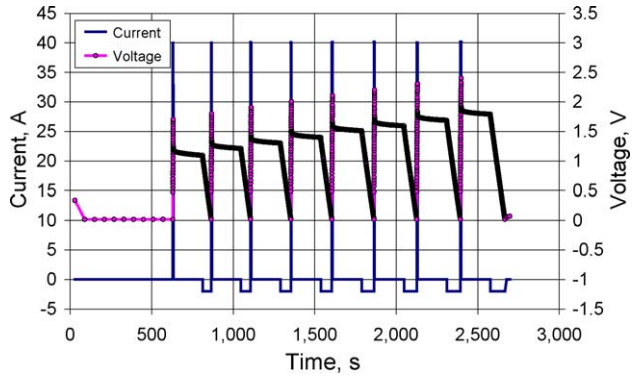

Fig. 2. Current and voltage profiles of the ACN-based capacitor at 45 °C. Starting from 0 V, the supercapacitor is charged at 40 A–1.7 V, held at open circuit for 180 s, and subsequently discharged to 0 V at 2 A. This sequence is repeated up to 2.5 V at 0.1 V increments.

−30 °C, there is a small reduction in specific energy, and the energy versus power curve is translated almost uniformly to a lower position relative to curves for the higher temperatures. At low power levels, the PC-based capacitor is not sensitive to temperature down to 0 °C. A reduction in performance is apparent at high power levels at 0 °C. At −30 °C, the performance of the PC-based capacitor suffers even at very low power levels, and the degree of reduction in stored energy increases significantly with increasing power.

We subsequently performed a series of energy tests to understand the underlying causes for the performance difference between the two supercapacitors. Fig. 2 shows the current and voltage profiles of the ACN-based capacitor at 45 °C. These profiles are representative of all other test results. A portion of the voltage profile is shown in Fig. 3, along with annotations that explain the approach used to assess the cell resistance. Analysis of the profile is based on an equivalent circuit consisting of a capacitor and a resistor connected in series. Although simple, this equivalent circuit has been used successfully to correlate supercapacitor behavior for a wide range of conditions [15]. At the beginning of a charging event, the instantaneous voltage drop (IR drop) can be used

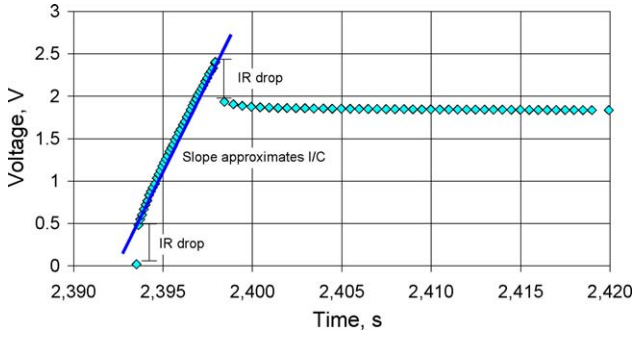

Fig. 3. Portion of the voltage profile in Fig. 1.The sharp voltage increase and drop at the beginning and the end of the 40 A charging steps, respectively, are due to IR (ohmic) losses. The voltage versus time profile during the charging step is approximated with a straight line, which allows for the estimation of the cell capacitance.

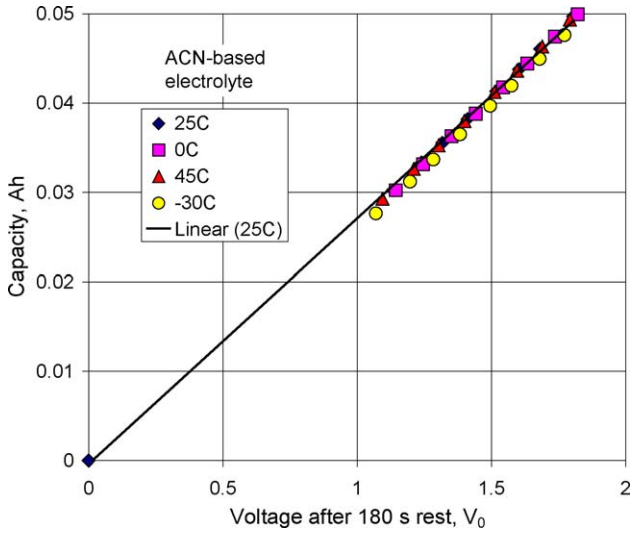

Fig. 4. Capacity measured using low-current discharge as a function of the equilibrium voltage after 180 s rest at open circuit for the ACN-based capacitor. The straight line reflects ideal capacitive behavior.

to estimate the resistance of the supercapacitor at 0 V. This resistance correlates well with the measured high-frequency resistance, often referred to as the equivalent series resistance (ESR). At the end of the charging event, the supercapacitor is allowed to equilibrate at open circuit for 180 s. The IR drop at the beginning of the open-circuit period can be used to estimate the resistance of the supercapacitor at that voltage or start of charge. The voltage versus time profile during the constant current charging process can be approximated with a straight line after a correction of the initial IR loss, and the slope of the line can be used to calculate the cell capacitance from the relation $C = I/(\mathrm{d}V/\mathrm{d}t)$. Note that this capacitance is obtained under a high current, which is relevant to practical applications. The open-circuit voltage V_0 at the end of the 180 s rest is interpreted as an equilibrium value. The subsequent low-current discharge to 0 V provides a measurement of the total charge stored in the supercapacitor. The (low current) cell capacitance is determined by dividing the total charge Q by V_0.

Figs. 4 and 5 summarize the coulombic capacity (in Ah) for both ACN and PC capacitors at four different temperatures. An ideal capacitor should display a linear relationship, including the origin, where $(Q,V_0) = (0,0)$. In this context, the behavior of the ACN-based capacitor closely resembles that of an ideal capacitor. Also of significance is the invariance in performance of the ACN-based capacitor with temperature. In contrast, Fig. 5 shows that the Q–V_0 relationship for the PC-based capacitor is nonlinear. While temperature seems to have a negligible effect from 45 to 0 °C, the PC-based capacitor suffers a significant reduction in stored charge at −30 °C.

Figs. 6 and 7 compare the capacitance–voltage relationship for ACN and PC supercapacitors. The effective capacitance of the ACN-based capacitor is insensitive to

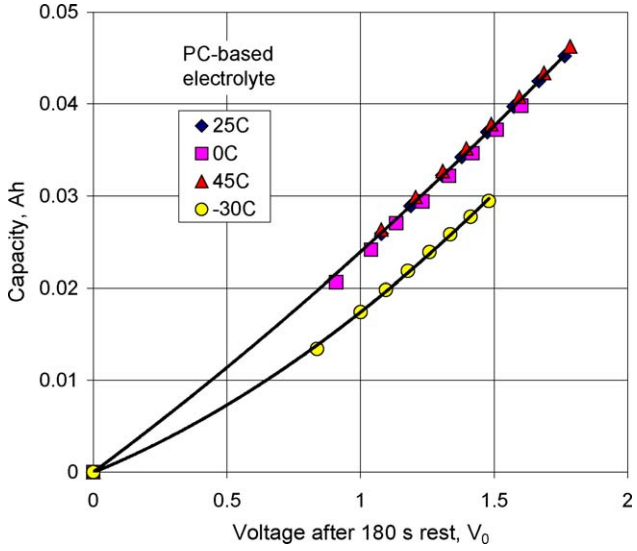

Fig. 5. Capacity measured using low-current discharge as a function of the equilibrium voltage after 180 s rest at open circuit for the PC-based capacitor. The nonlinear relationship particularly evident at low temperatures reflects deviation from the ideal capacitive behavior.

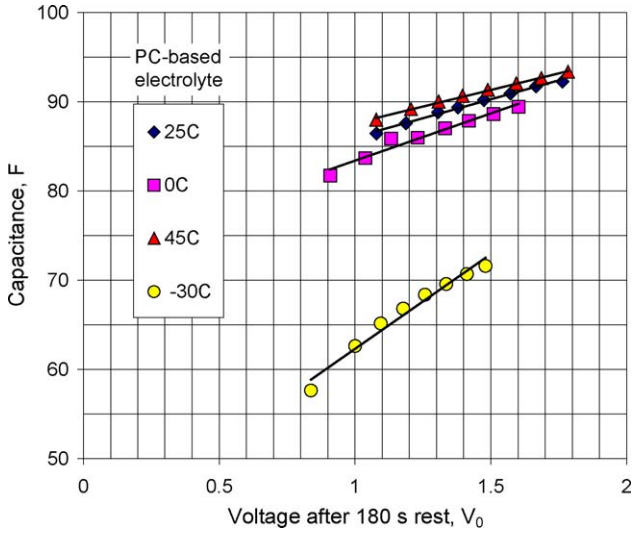

Fig. 7. Capacitance extracted from low-current discharge as a function of equilibrium voltage for the PC-based supercapacitor. The line corresponding to the −30 °C data has a very large slope, reflecting a strong dependence of capacitance on voltage. Relative −30 °C data, the temperature dependence is less pronounced at higher temperatures, but a greater dependence on temperature is seen for the PC-based cell than that of the ACN-based cell.

temperature while that of the PC-based capacitor suffers significant reduction at −30 °C. The capacitance of the ACN-based capacitor varies linearly with voltage with a slope of 5.2 F/V at −30 °C. The linear relationship is also applicable to the PC-based capacitor, although the PC-based capacitor exhibits much larger slopes of 10.6 and 21.2 F/V at 0 and −30 °C, respectively.

The variation of capacitance of carbon electrodes with voltage has been discussed in detail in the literature. For example, Hahn et al. [16] showed an asymmetric, parabolic-shaped capacitance–voltage curve for an activated-carbon

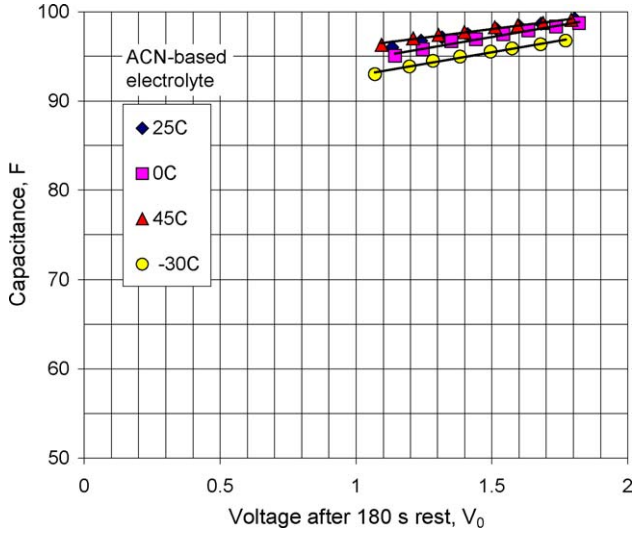

Fig. 6. Capacitance extracted from low-current discharge as a function of equilibrium voltage for the ACN-based supercapacitor. The data reflect a weak dependence of capacitance on voltage.

electrode with a tetrethylammonium tetrafluoroborate–ACN electrolyte. The minimum capacitance is observed at the point-of-zero-charge (pzc) potential. In a complete (symmetric) carbon-carbon supercapacitor, the two electrodes will share the applied voltage with opposite sign. Consequently, capacitance would be expected always to increase with voltage. Hahn et al. [16] attributed the strong variation of capacitance with voltage to contributions from space-charge capacitance within carbon. This argument may be valid when basal planes of graphite dominate the carbon–electrolyte interface. On the edge planes, graphite is regarded as a metal, and the double-layer capacitance is determined by the Helmholtz layer and solution-phase characteristics [17]. The small variation of capacitance with voltage for the ACN-based capacitor is not consistent with the posited space-charge argument. For completeness, it should also be recognized that larger potentials can lead to Faradaic reactions, including Faradaic adsorption processes, and these phenomena could lead to an increase in capacitance with increasing voltage as seen in Figs. 6 and 7.

Table 1 summarizes the capacitances of the PC and ACN capacitors estimated from the slope of the voltage–time profiles at high currents and the capacitances calculated from the low-current (coulomb integration) experiments. Not surprisingly, the high-current capacitance is systematically lower than the low-current capacitance, although the extracted values for the capacitance show good agreement. For the PC-based capacitor, the difference is more pronounced at −30 °C, at which the rate capability of the supercapacitor is compromised as shown earlier in the Ragone plots; this observation is consistent with the fact that the viscosity of PC increases more rapidly than that of ACN at low temperatures, resulting

Table 1
Capacitances of PC and ACN capacitors measured from high-current experiments (cf. Fig. 3) and values calculated from the low-current discharge capacities

Temperature (°C)	Propylene carbonate		Acetonitrile	
	Capacitance from high current (F)	Low-current capacitance (F)	Capacitance from high current (F)	Low-current capacitance (F)
−30	63.0	71.6	93.1	96.8
0	87.7	89.4	94.4	98.7
25	90.1	92.3	93.5	99.2
45	91.4	93.4	92.3	99.1

in a greater decline in the ionic conductivity in the case of PC.

Figs. 8 and 9 display the variation of interrupt resistance with voltage and temperature. At 25 and 45 °C, the resistance of the ACN-based capacitor (∼12 mΩ) is slightly smaller than that of the PC-based capacitor (∼16 mΩ). The difference in resistances is larger at lower temperatures. While the values for the ACN-based capacitor remain quite stable (12 and 14 mΩ for 0 and −30 °C, respectively), the values for the PC-based capacitor increase significantly to 25 and 77 mΩ for 0 and −30 °C, respectively. For both the solvent systems, the cell resistance is independent of the state-of-charge, which is in contrast to several previous reports. We have recently shown that the resistance of a carbon-based supercapacitor made by SAFT decreases linearly with voltage from 0 to 2.5 V at 25 °C [15]. Kastening et al. [18] observed a similar correlation. Hahn et al. [16] recently made similar observations with respect to resistance variation with voltage, and explained the variation by considering graphite as a conductor with a finite density of states at the Fermi level as alluded to above.

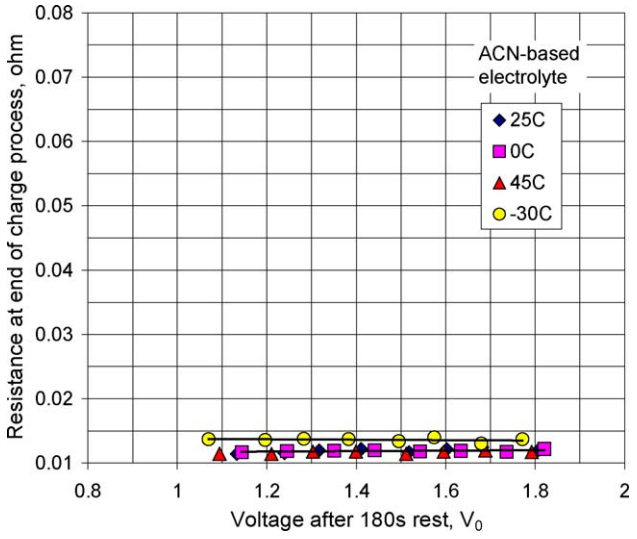

Fig. 8. Interrupt resistance measured at the end of the charging step as a function of the equilibrium voltage after a 180 s open-circuit stand for the ACN-based capacitor.

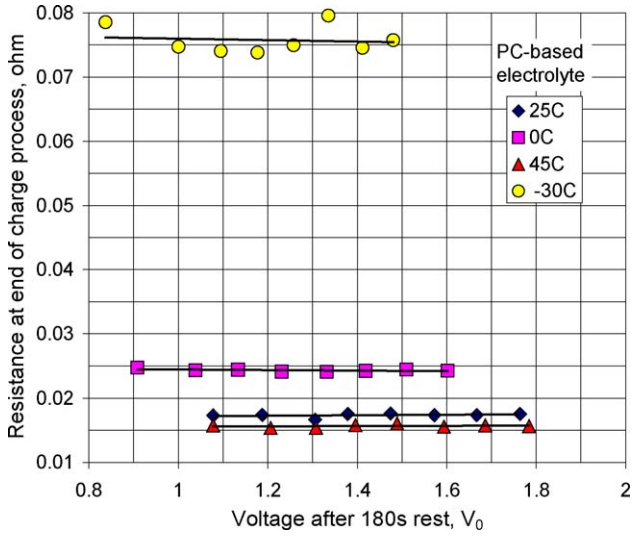

Fig. 9. Interrupt resistance measured at the end of the charging step as a function of the equilibrium voltage after a 180 s open-circuit stand for the PC-based capacitor.

Arrhenius plots are constructed based on the supercapacitor resistance at 0 V (Fig. 10). Within the temperature range of this study, the ACN-based capacitor exhibits a linear Arrhenius relationship with an activation energy of 1.90 kJ mol^{-1}. The PC-based capacitor, however, shows a nonlinear relationship. At temperatures below ambient (lower than 12 °C), a linear Arrhenius relationship can be identified. Above that temperature range, the resistance is largely insensitive to temperature. The activation energy estimated based on the low-temperature range data is 16 kJ mol^{-1}. This evolution of resistance with temperature is consistent with a recent report on a 2700 F supercapacitor [4]; unfortunately, the identity of the supercapacitor was not revealed and an empirical polynomial expression was used without any explanation of the underlying causes.

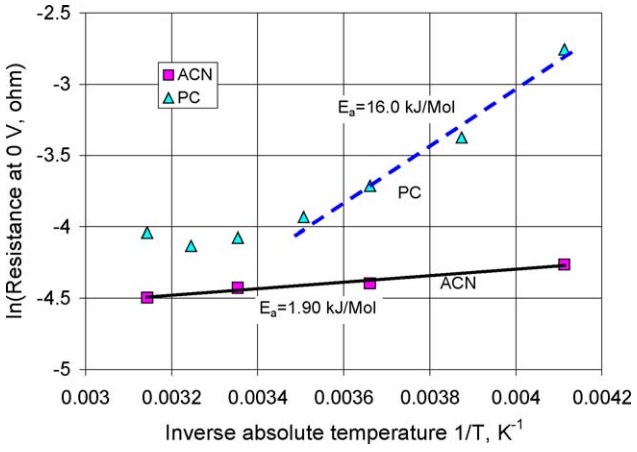

Fig. 10. Arrhenius plots for the ACN and PC-based capacitors based on the interrupt resistance at 0 V. Activation energies (E_a) are calculated from the slope of the curves.

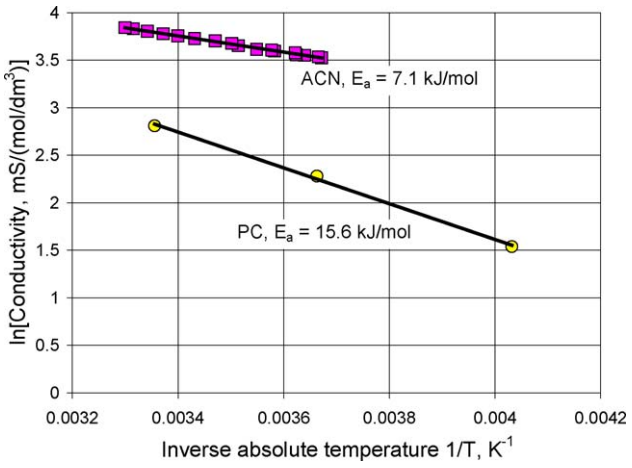

Fig. 11. The Arrhenius plots for tetraethylammonium tetrafluoroborate in ACN and PC. The conductivity is normalized to solution concentration.

The implications of the activation energies for ACN and PC capacitors can be better understood by comparing them to the values for electrolytes used in the supercapacitors. Fig. 11 shows conductivity data obtained from the literature [19,20]. The salt in the electrolyte is 1 M tetraethylammonium tetrafluoroborate. The activation energies for ACN and PC electrolytes are 7.08 and 15.0 kJ mol^{-1}, respectively. We also note that the viscosity of PC and ACN are 2.513 and 0.369 Pa s^{-1}, respectively [21]. The activation energy for the ACN-based capacitor is much smaller than that of the electrolyte. This fact indicates that the resistance of the electrolyte does not dominate the resistance of the ACN-based capacitor. Instead, it is more likely to be determined by the resistance of the carbon electrode (although we cannot rule out the contact resistance at the carbon-aluminum interface).

For the PC-based capacitor, the activation energy at low temperatures is very close to that of the electrolyte, indicating that in the temperature range −30 to 12 °C, the resistance of the supercapacitor is dominated by the electrolyte. At higher temperatures, however, the insensitivity of the resistance to temperature indicates that the solid phase of the carbon electrode controls the cell impedance.

4. Conclusions

We compare the electrochemical performance of two electrical-double layer supercapacitors employing electrolytes of acetonitrile (ACN) or propylene carbonate (PC) with tetraethylamononium tetrafluoroborate. In the temperature range of interest for automotive traction applications (−30 to 45 °C), the capacitance and resistance of the two capacitors are deduced from electrochemical data. Both values for the ACN-based capacitor are insensitive to temperature, in contrast to the PC-based capacitor. The activation energy for the ACN-based capacitor, extracted from cell resistance data, is lower than that of the ACN-based electrolyte, indicating that components other than the electrolyte control the cell resistance. A plausible explanation for this observation is that resistance to electron transport in the porous carbon phase dominates the resistance of ACN-based capacitors. In contrast, similar activation energies are observed for the PC-based capacitor and electrolyte below ambient temperature, indicating that the resistance of the electrolyte is responsible for the high resistance of the capacitor at low temperatures and its relatively poor low-temperature electrochemical performance. The outstanding low-temperature performance of the ACN-based supercapacitors makes them very attractive for automobile applications, and it would seem likely that vehicle integration efforts should be considered in order to ensure appropriate abuse tolerance for the ACN-based energy-storage system.

Acknowledgement

We would like to express our thanks to Nesscap Co., Ltd., for providing the supercapacitor samples.

References

[1] A. Burke, J. Power Sources 91 (2000) 37–50.
[2] M.W. Verbrugge, Supercapacitors and Automotive Applications, in: Proceedings Volume for the *World Summit on Advanced Capacitors*, Washington, DC, 2003.
[3] A. Chu, P. Braatz, J. Power Sources 112 (2002) 236.
[4] H. Gualous, D. Bouquain, A. Berthon, J.M. Kauffmann, J. Power Sources 123 (2003) 86.
[5] J.P. Zheng, Z. Jiang, Proceedings Volume for the Electrochemical Society Meeting, Honolulu, HI, 2004, Abstract No. 680.
[6] C. Portet, P.L. Tabena, P. Simon, C. Laberty, Electrochim. Acta 49 (2004) 905–912.
[7] Y.P. Guo, J.R. Qi, Y.Q. Jiang, S.F. Yang, Z.C. Wang, H.D. Xu, Mater. Chem. Phys. 80 (2003) 704.
[8] X.W. Huang, Z.W. Xie, X.Q. He, H.Z. Sun, C.Y. Tong, D.M. Xie, Synth. Met. 135–136 (2003) 235.
[9] Yoo Jeeyoung, Kim Kyungho, Kim Jaekun, Yeu Taewhan, Proceedings Volume for the Electrochemical Society Meeting, Honolulu, HI, 2004, Abstract No. 677.
[10] M. Arulepp, L. Permann, J. Leis, A. Perkson, K. Rumma, A. Jänes, E. Lust, J. Power Sources 133 (2004) 320–328.
[11] E. Lust, A. Jänes, M. Arulepp, J. Electroanal. Chem. 562 (2004) 33–42.
[12] E. Lust, A. Jänes, M. Arulepp, J. Solid State Electrochem. 8 (2004) 488–496.
[13] A. Jänes, L. Permann, M. Arulepp, E. Lust, J. Electroanal. Chem. 569 (2004) 257–269.
[14] B.E. Conway, Electrochemical Supercapacitors, Scientific Fundamentals and Technological Applications, Kluwer Academic/Plenum Publishers, 1999, pp. 644–648.
[15] M.W. Verbrugge, P. Liu, S. Soukiazian, J. Power Sources 141 (2005) 369.
[16] M. Hahn, M. Baertschi, O. Barbieri, J.-C. Sauter, R. Kötz, R. Gallay, Electrochem. Solid State Lett. 7 (2004) A33.
[17] B.E. Conway, Electrochemical Supercapacitors, Scientific Fundamentals and Technological Applications, Kluwer Academic/Plenum Publishers, 1999, pp. 193–196.

[18] B. Kastening, M. Hahn, B. Rabanus, M. Heins, U. zum Felde, Electrochim. Acta 42 (1997) 2789.
[19] B.E. Conway, Electrochemical Supercapacitors, Scientific Fundamentals and Technological Applications, Kluwer Academic/Plenum Publishers, 1999, p. 373.
[20] Yu.A. Malentin, A.A. Mironova, L.B. Koval, V.V. Danilin, Ukr. Khim. Zhurn. 67 (2001) 6.
[21] R.L. David, H.P.R. Frederisce (Eds.), CRC Handbook of Chemistry and Physics, 73rd ed., CRC Press, New York, 1995.